3B2v8.06a/w (Dec 5 2003).51c XML:ver:5.0.1 CRYS : 13868 Prod.Type:COM pp.1–7(col.fig.:1–4) ED:SudhirKumarM. PAGN:gopal SCAN:mdali

ARTICLE IN PRESS

ELSEVIER

Available online at www.sciencedirect.com

SCIENCE DIRECT®

Journal of Crystal Growth ▮ (▮▮▮▮) ▮▮▮–▮▮▮

JOURNAL OF CRYSTAL GROWTH

www.elsevier.com/locate/jcrysgro

The influence of vibration on hydrodynamics and heat-mass transfer during crystal growth

Alexey Fedyushkin[a,*], Nicolai Bourago[a], Vadim Polezhaev[a], Evgenii Zharikov[b]

[a]*Institute for Problems in Mechanics of RAS, 119526, Vernadskogo101/1, Moscow, Russia*
[b]*Institute of General Physics of RAS, Moscow, Russia,*

Abstract

The results of mathematical and physical modeling of heat and mass transfer in vibrating flows are presented for Bridgman crystal growth with submerged vibrator. A shadow graphic system and computer processing of photographs is used to observe the melt motion in the experiments. Mathematical modeling is performed on the basis of the unsteady Navier–Stokes–Boussinesq equations for incompressible fluid including the Stefan boundary condition at the melt–crystal interface. The finite element code ASTRA was used for calculations. In numerical simulation the calculated instantaneous flows were averaged in time to evaluate the averaged vibrational flow (AVF).

The results of research about the influence of high-frequency vibrations with small amplitudes on hydrodynamics and heat transfer are reported. The numerical and experimental results illustrate the influence of the vibration on the AVF, on the temperature distribution and on the curvature of the crystallization front.

PACS: 44.27.+g; 47.27.Te; 47.11.+j; 47.62.+q

Keywords: A1. Computer simulation; A1. Fluid flow; A1. Heat transfer; Interfaces; A1. Vibration; A2.Bridgman technique

1. Introduction

In the present paper the influence of the vibrations on the melt flow is considered for the vertical Bridgman crystal growth. The vibrations are initiated by a submerged vibrator. It should be mentioned that a large variety of different vibrations exists [1]. We consider here progressive vertical vibrations induced by the submerged vibrating disk Fig. 1a. The applied vibrations are assumed to be of small amplitude, therefore the vibrator displacements are negligible, and the velocity of the vibrator is predefined as a harmonic function $v = A\omega \sin(\omega t)$v = awsin , where A—an amplitude, ω—a frequency. Some of the results were calculated on the basis of the direct solution of the axisymmetrical unsteady Navier–Stokes–-

*Corresponding author. Tel.: +7 095 434 3283; fax: +7 095 938 2038.
E-mail address: fai@ipmnet.ru (A. Fedyushkin).

0022-0248/$ - see front matter © 2004 Elsevier B.V. All rights reserved.
doi:10.1016/j.jcrysgro.2004.11.220

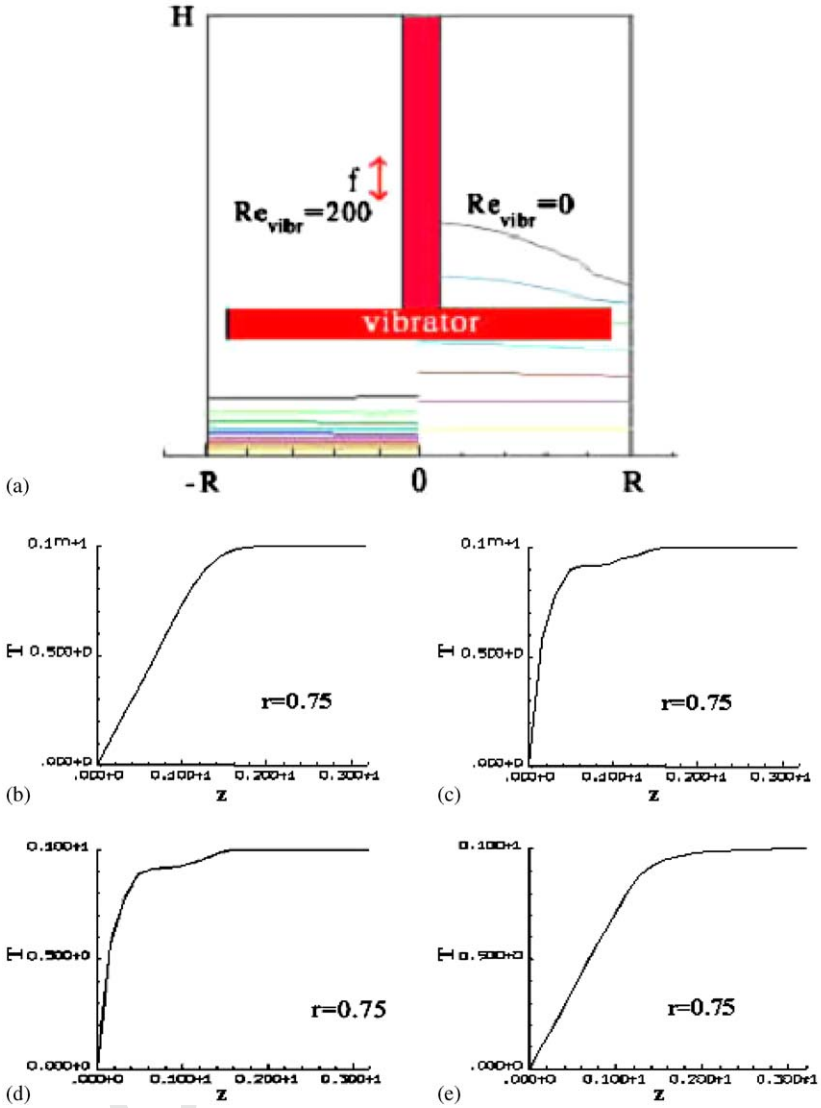

Fig. 1. Influence of vibration on temperature field. (a) Isotherms in the melt for two cases: with (left) and without (right) vibration, (b–e) vertical temperature profile for four sets of parameters: (b) $Re_{\mathrm{vibr}} = 0$ (without vibration), $Gr = 2 \times 10^6$, $Pr = 5.43$, (c) $Re_{\mathrm{vibr}} = 200$ ($f = 50\,\mathrm{Hz}$), $Gr = 2 \times 10^6$, $Pr = 5.43$, (d) $Re_{\mathrm{vibr}} = 200$, $Gr = 0$, $Pr = 5.43$, (e) $Re_{\mathrm{vibr}} = 200$, $Gr = 2 \times 10^6$, $Pr = 0.01$.

Boussinesq problem, while some were obtained in the physical experiments by using the laser shadow graphic method. It is known that under influence of vibrations the averaged in time flows appear [1]. In the present paper,we named these averaged vibrational flow as AVF. Such flows very often are observed by experimentators in the liquids under the influence of vibrations. A lot of issues should be taken into account to get a deep understanding of the mechanisms acting on the AVF. Here only some of them are in question. In particular, the following features are under study here: influence of vibrations on the boundary layers in melts with various Prandtl numbers; influence of frequency of the vibrations on the structure of the AVF; influence of the amplitude of the vibrations on

the shape of the solid–liquid interface; influence of the arrangement of the vibrator and crucible on the AVF; and, finally, the influence of the rotation on the AVF. The presented results should be treated as preliminary by far is complete. We are just making first steps on the way to understanding the possible outcomes from using the vibrations as a handling tool in the crystal growth production techniques.

2. Statement of the problem

Numerical modeling of hydrodynamics and heat-mass transfer for the Bridgman system with submerged vibrator sketched in Fig. 1a was conducted on the basis of the unsteady axisymmetrical 2D Navier–Stokes–Boussinesq equations including the balance equations for heat and mass transfer

$$\frac{\partial u}{\partial r}+\frac{u}{r}+\frac{\partial w}{\partial z}=0, \tag{1}$$

$$\frac{\mathrm{d}u}{\mathrm{d}t}-\frac{v^2}{r}=-\frac{1}{\rho}\frac{\partial p}{\partial r}+\frac{1}{r}\frac{\partial}{\partial r}\left(r\nu\frac{\partial u}{\partial r}\right)+\frac{\partial}{\partial z}\left(\nu\frac{\partial u}{\partial z}\right)-\nu\frac{u}{r^2}, \tag{2}$$

$$\frac{\mathrm{d}w}{\mathrm{d}t}=-\frac{1}{\rho}\frac{\partial p}{\partial z}+\frac{1}{r}\frac{\partial}{\partial r}\left(r\nu\frac{\partial w}{\partial r}\right)+\frac{\partial}{\partial z}\left(\nu\frac{\partial w}{\partial z}\right)+g\beta(T-T_0), \tag{3}$$

$$\frac{\mathrm{d}v}{\mathrm{d}t}+\frac{uv}{r}=\frac{1}{r}\frac{\partial}{\partial r}\left(r\nu\frac{\partial u}{\partial r}\right)+\frac{\partial}{\partial z}\left(\nu\frac{\partial u}{\partial z}\right)-\nu\frac{u}{r^2}, \tag{4}$$

$$\frac{\mathrm{d}\rho c_\mathrm{p}T}{\mathrm{d}t}=\frac{1}{r}\frac{\partial}{\partial r}\left(r\lambda\frac{\partial T}{\partial r}\right)+\frac{\partial}{\partial z}\left(\lambda\frac{\partial T}{\partial z}\right), \tag{5}$$

$$\frac{\mathrm{d}C}{\mathrm{d}t}=\frac{1}{r}\frac{\partial}{\partial r}\left(rD\frac{\partial C}{\partial r}\right)+\frac{\partial}{\partial z}\left(D\frac{\partial C}{\partial z}\right). \tag{6}$$

The boundary conditions readat the axis of symmetry:

$$(r=0): u=0,\quad \frac{\partial w}{\partial r}=0,\quad v=0,\quad \frac{\partial T}{\partial r}=0,\quad \frac{\partial C}{\partial r}=0; \tag{7}$$

at the solid–liquid interface $u=0$, the location and velocity W_S are determined in view of Stefan condition:

$$\rho L W_\mathrm{s}=\lambda\frac{\partial T}{\partial n_\mathrm{melt}}-\lambda_\mathrm{cryst}\frac{\partial T}{\partial n_\mathrm{cryst}},\quad T=T_\mathrm{m},\quad v=2\pi r\Omega_\mathrm{C},\quad D\frac{\partial C}{\partial z}=W_\mathrm{S}C(1-k_0); \tag{8}$$

at side wall of crucible:

$$r=R: u=0,\quad w=0,\quad v=2\pi R\Omega_\mathrm{C}, \tag{9}$$

$$\frac{\partial T}{\partial r}=0(0<z<h),\quad T=T_h(h<z<H),\quad \frac{\partial C}{\partial r}=0; \tag{10}$$

at vibrator:

$$u=0,\quad w=A\omega\sin(\omega t),\quad v=2\pi r\Omega_\mathrm{vibr},\quad \frac{\partial C}{\partial n}=0,\quad \frac{\partial T}{\partial n}=0 \tag{11}$$

at the upper opened boundary:

$$(z=H),\quad u=0,\frac{\partial w}{\partial z}=0,\quad v=0,\quad T=T_\mathrm{h},\quad C=C_0. \tag{12}$$

Initial conditions:

$$t=0: u=0,\quad w=0,\quad v=0,\quad T=T_\mathrm{m},\quad C=C_0. \tag{13}$$

Hereafter the following notations are used: r and z—radial and axial coordinates, t—time, u and w—velocity vector components in r and z directions, v—azimutal velocity, T—temperature, C—dopant concentration, p—pressure, ρ—density, g—gravity acceleration, β_T, ν, λ, λ_cryst, c_p, D—coefficients of thermal expansion, kinematic viscosity, heat conductivity, heat capacity and dopant diffusivity, A and ω—amplitude and frequency of vibrations, Ω—angular velocity of the rotating crucible, a—thermal conductivity coefficient, W_s—normal rate of the crystal growth, R—radius of crucible is scale of length, $\Delta T=T_\mathrm{max}-T_\mathrm{min}$—temperature scale, k_0—dopant segregation factor, n—normal unity vector, and L—latent heat of crystallization. The dimensionless coordinates, velocity, time and temperature are calculated with the following expressions:

$$r' = r/R, \quad z' = z/R, \quad u' = uR/n,$$
$$t' = tn/R^2, \quad T' = (T - T_{\min})/\Delta T.$$

All calculations were conducted for the initial temperature field, which corresponds to the thermal regimes with temperature boundary conditions given above.

In the present paper the results received from the numerical simulation of two crystallization models are presented: (1)with a flat surface of the melt–crystal interface and (2)with the determination of the melt–crystal interface from the solution of the Stefan task. In the second case, the temperature in the crystal was determined from the solution of the additional equation of heat conductivity for the crystal. The basic accounts were carried out on the first model and the second model was used only for research of the influence of vibrations on the shape of the crystallization front. In the first case, the crystal growth rate was the same in all runs: $W_s = 0.3\,\text{cm/h}$ at $z = 0$. The amplitude of vibrations was constant $A = 100\,\mu\text{m}$. The problem is characterized by the following similar numbers: rotational Reynolds number $Re_\Omega = \Omega_C R^2/\nu$, Reynolds number $Re = W_s R/\nu$, vibrational Reynolds number $Re_{\text{vibr}} = A\omega R/\nu$, Grashof number $Gr = g\beta\,\Delta T R^3/\nu^2$, (or Rayleigh number $Ra = Gr\,Pr$), Prandtl number $Pr = \nu\rho c_p/\lambda$ and Schmidt number $Sc = \nu/D$.

3. Numerical and experimental results

The initial boundary value problem (1–13) was solved by the finite element method by using the code ASTRA [2,3].

It is known [1], that under the effect of vibrations, two types of the flow can be selected depending on the time scale: instantaneous vibrational flow and AVF. These flows can lead to significant additional mixing and redistribution of the temperature and dopant [1,4,5].

3.1. Influence of vibrations on boundary layers

In Fig. 1 the temperature distribution in the melt with ($Re_{\text{vibr}} = 200$) and without vibration is illustrated. In Fig. 1b 4 dimensionless values are designated without apostrophes. Fig. 1a shows isotherms in the melt and Figs. 1b–e show the calculated vertical temperature profiles ($r = 0.75$) for the following four cases: (a)thermal convection without vibrations, (b)thermal convection with vibrations under high Prandtl number ($Gr = 2 \times 10^6$, $Pr = 5.43$), (c)vibrational flow without thermal convection ($Gr = 0$, $Pr = 5.43$), (d)thermal convection with vibrations under low Prandtl number ($Gr = 2 \times 10^6$, $Pr = 0.01$). These results show that the vibrations strongly decrease the thickness of the temperature boundary layers (Fig. 1b and c). The results show that the influence of the vibrations on the temperature in terrestrial and microgravity environment is practically the same, i.e. the effects of the vibrations and the gravity are practically independent. Of course, the influence of the vibrations on the temperature field depends on the amplitude and the frequency of the vibrations, on the heat conductivity and the viscosity (on the Prandtl numbers).

The temperature field in the case for $Pr = 0.01$ as well as in the case of microgravity is practically not changed by the vibrations (Fig. 1e). In such a case, where Prandtl numbers are low, the vibrations of increased amplitude and frequency should be applied to get the effect of thin boundary layers.

3.2. Influence of vibration frequency on the AVF

Some special feature of the influence of the frequency on the AVF was detected in the calculations, with increase of frequency the AVF can change its direction. This is shown in Fig. 2, which presents the AVF stream function isolines for $A = 100\,\mu\text{m}$, $Gr = 2\ 106$, $Pr = 5.43$ and four values of vibrational Reynolds number (frequency): (a) $Re_{\text{vibr}} = 40$ ($f = 10\,\text{Hz}$), (b) $Re_{\text{vibr}} = 120$ ($f = 30\,\text{Hz}$), (c) $Re_{\text{vibr}} = 200$ ($f = 50\,\text{Hz}$), (d) $Re_{\text{vibr}} = 400$ ($f = 100\,\text{Hz}$). With increase in number Re_{vibr} near the vibrator there are secondary vortexes (with agreed directions of rotation) with a further increase of Re_{vibr} a dominant vortex becomes a vortex with an opposite direction. For example, with increase of the frequency (vibrational Reynolds number Re_{vibr}) from $f = 10\,\text{Hz}$ up to $f = 100\,\text{Hz}$ the intensity of the AVF also grows, while the AVF direction changes due to exchange

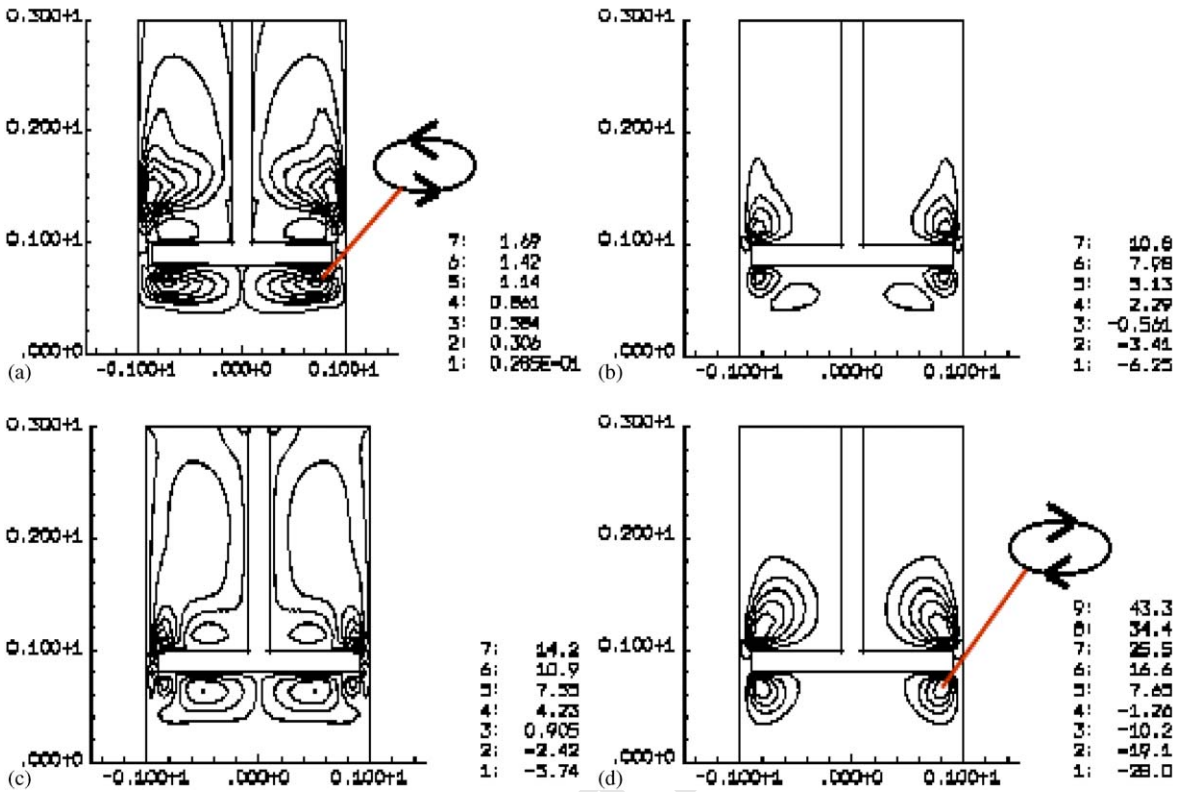

Fig. 2. Influence of vibrational Reynolds number (frequency) on AVF. ($A = 100\,\mu$m, $Gr = 2 \times 10^6$, $Pr = 5.43$), (a) $Re_{vibr} = 40$ ($f = 10$ Hz), (b) $Re_{vibr} = 120$ ($f = 30$ Hz), (c) $Re_{vibr} = 200$ ($f = 50$ Hz), (d) $Re_{vibr} = 400$ ($f = 100$ Hz).

of momentum between vortexes. The direction of the AVF changes from clockwise at $Re_{vibr} = 40$ ($f = 10$ Hz) (Fig. 2a) to anticlockwise at $Re_{vibr} = 400$ ($f = 100$ Hz) (Fig. 2d) (negative values of the AVF stream function correspond to the clockwise flow). The fight between the convective and vibrational vortexes can be observed. Under the vibrator the thermal convective flow has anticlockwise direction, while the AVF has opposite direction. It can be expected that this fight can essentially effect the dopant distribution and the shape of the solid–liquid interface.

3.3. Influence of amplitude on shape of melt–crystal interface

The influence of the amplitude on the shape of the solid–liquid interface is shown in Fig. 3. These data were obtained experimentally by Prof. E.V. Zharikov's group. In the experiments $NaNO_3$ crystals were grown in quartz ampoules ($R = 1$ cm, $H = 3$ cm) with rate of crystallization of 0.3 cm/h. The conditions of growth were identical at the changing of the frequency—peak characteristics. The influence of the anisotropic of heat conductivity of $NaNO_3$ on the shape of crystallization front was not investigated and in the numerical model, the heat conductivity was constant.

On the left-handside of Fig. 3 the photographs of the grown crystals are shown, and on the right-hand side the patterns of melt flows are shown, which were observed in the experiments. The vertical progressive harmonic vibrations had a frequency 50 Hz and amplitudes in the interval of 180–220 μm ($Re_{vibr} = 300 - 480$). By varying the

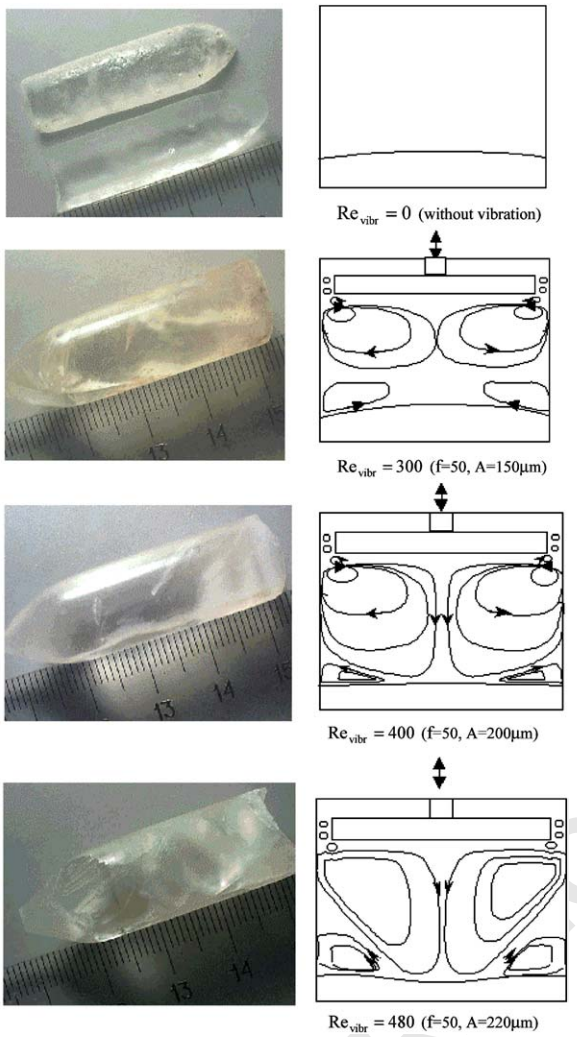

Fig. 3. Influence of vibration on the shape of melt–crystal interface (experimental data): at the left-handside of the figure are the images of Ag: $NaNO_3$ single crystals grown under and without of vibrations; at the right-handside of the figure are the corresponding flow patterns in the melt and shape of melt–crystal interface.

amplitude it is possible to effect the curvature of the solid–liquid interface.

In Fig. 4 the results of numerical modeling are submitted. The stream function of instant and averaged flows, and the isotherms are shown for two cases: at the left without vibrations, and on the right with vibration ($Re_{\mathrm{vibr}} = 200$).

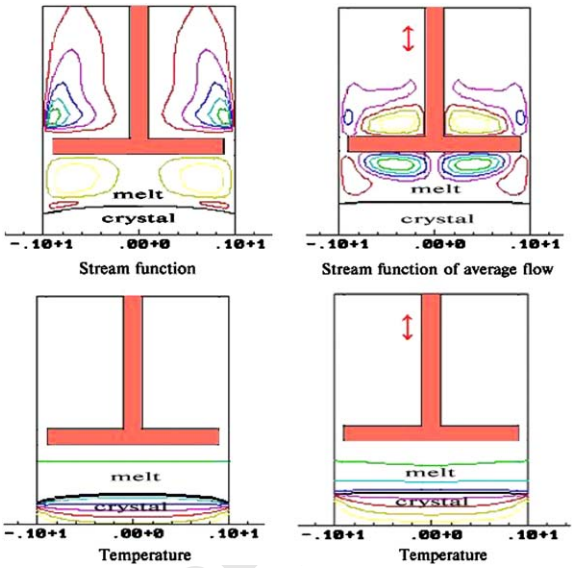

Fig. 4. Influence of vibration on the shape of melt–crystal interface (results of numerical modeling). At the left-handside—without vibration, at the right-handside—with vibration ($Re_{\mathrm{vibr}} = 200$).

The given results are in good agreement qualitatively with the experimental data (Fig. 3). Thus it is experimentally and numerically shown that the vibrations can flatten the crystallization front. This fact looks quite promising for controlling of the melt–crystal shape during crystal growth.

4. Conclusions

The researches of distribution of an impurity have shown that it is similar to distribution of the temperature. The concentration boundary layers are subject more to the influence of vibrations only, because of the usual numbers $Sc > 10$.

The vibrations can decrease the thickness of the boundary layers at the solid–liquid interface. It is shown that by applying the vibrations the temperature and concentration gradients near the solid–liquid interface, the crystal growth rate and the AVF flow direction can be changed and also that the vibrations can flatten the crystallization front. We see the possibility that the kinetics of

growth and growth rate can be influenced by vibration.

The study shows that the vibrations can be used as a simple and effective controlling tool, to improve the conditions of crystal growth and the quality of the final product.

5. Uncited reference

[6].

References

[1] G.Z. Gershuni, D.V. Lubimov, Thermal Vibrational Convection, Willey, New York, 1998 357p.
[2] N.G. Bourago, Lectures of FEM-94 Seminar, Chalmers University of Technology, Gothenburg, 1994, pp. 1–15.
[3] N.G. Bourago, A.I. Fedyushkin, V.I. Polezhaev, Proceedings of joint Tenth European and Sixth Russian Symposium on Physical sciences in microgravity. St. Peterburg, Russia, vol. II, 1997, pp. 170–173.
[4] A.I. Fedyushkin, N.G. Bourago, Proceedings of Second Pan Pacific Basin Workshop on Microgravity Sciences 2001, paper CG-1065, 9p.
[5] A.I. Fedyushkin, N.G. Bourago, Proceedings of Second Pan Pacific Basin Workshop on Microgravity Sciences, 2001, paper CG-1073, 11p.
[6] N.G. Bourago, V.N. Kukudzhanov, Computer Mechanics of Solids, Nauka, Mascow, 1991, pp. 78–122.